Field experiment on the dynamics of fine sediments over a gravel bar in an alpine gravel-bed river

B. Camenen, A. Herrero, Guillaume Dramais, F. Thollet, C. Le Bescond, E. Perret, Céline Berni

9th symposium on river, coastal and estuarine morphodynamics, RCEM, Iquitos City, Peru, 30 August - 03 September, 2015

Field experiment on the dynamics of fine sediments over a gravel bar in an alpine gravel-bed river

B. Camenen[1]*, A. Herrero[1], G. Dramais[1], F. Thollet[1], C Le Bescond[1], E. Perret[1], C. Berni[1]

[1] Irstea, UR HHLY, Lyon-Villeurbanne Center, Villeurbanne, France
* benoit.camenen@irstea.fr

1. Introduction

Alpine gravel-bed rivers are often characterized by very poorly sorted sediments and significant grain sorting is observed on gravel bars with relatively coarse sediments on the bar head and transverse channel and fine sediments on the bar tail (Lisle et al., 1991; Diplas, 1994; Lanzoni, 2000; Eekhout et al., 2013). The grain size variability significantly influences the inception of movement for each of the classes represented over a gravel bar (Konrad, 2002). In particular, fine sediment infiltration in the bed and fine sediment deposits are often observed over gravel bars in alpine rivers (Diplas, 1994; Lisle and Hilton, 1999). Depending on the fine sediment content, fine sediments may limit or enhance gravel mobility (Diplas and Parker, 1992). The purpose of this paper is to present some field measurements performed on the Arc en Maurienne River, France. Main objectives are to characterize the dynamics of fine sediment infiltration in the gravel matrix for conditions close to the incipient motion of gravels. The field campaign was carried out on a gravel bar located 10 km downstream of St Jean de Maurienne during the dam flushing event on June 17th, 2014, where patches with clean gravels were previously built. Water surface levels and surface velocities were measured during the event as well as sediment concentrations. Volume and characteristics of the sediment infiltrated in the patches were estimated after the event. A discussion of the impact of this event on the infiltration dynamics is provided.

2. Experimental site and data

2.1 Location of the experimental site

The fieldwork took place in the Arc River, located in the French Alps. The catchment area is 1957 km^2 (grey area in Fig. 1) with a nival hydrologic regime and a mean water discharge from 6-8 m^3/s in winter to 15-20 m^3/s in summer (Jodeau, 2007; Jaballah, 2013). The river bed has been largely modified and artificially straightened in many places in order to allow the 1 km wide valley to contain a road, a highway and a railway. In addition the flow is regulated by many hydraulic constructions (several dams and pipes) for hydroelectricity production. The present regulated flow regime has significantly altered the natural river discharges and sediment transport. Although its bed is made of gravel, the Arc en Maurienne River is characterised by high fine sediment transport (black Lias schist mainly), supplied by tributaries (such as the Arvan and Glandon streams). The area of interest is located in a system of alternate bars 18 km from the downstream reservoir at Sainte-Marie-de-Cuines (see Fig. 1). This system is apparently forced due to the presence of a bend and a bridge pier at the downstream boundary (Jaballah et al., 2014). Lateral limits are set by 5 m high embankments made of boulders and scattered young trees leading to a river width of 50 m in average. The mean slope of this reach is approximately 0.6%. More precisely, the fieldwork was carried out on a gravel bar located on the left side of the river 2.5 km upstream the confluence with the Glandon tributary (2 km upstream the bridge).

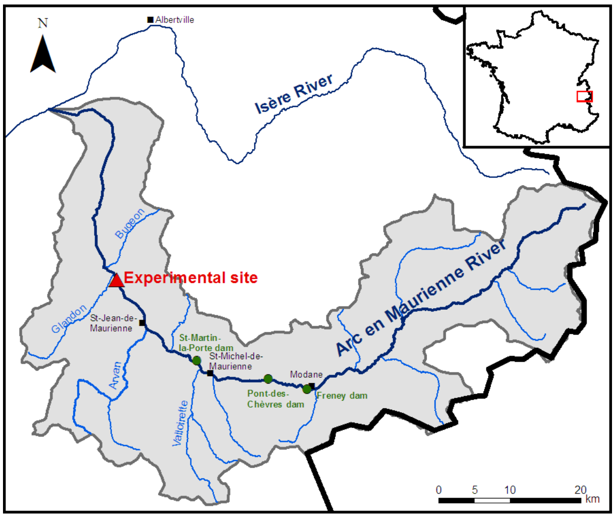

Figure 1: Map of the study site (green circles correspond to the three river dams).

2.2 Experimental set-up

A procedure is proposed here to study infiltration of fine sediments in a matrix made of gravel particles. Two patches were built on a gravel bar, which separates a secondary channel from the main channel, using gravels of 4 to 10 cm in diameter (see Fig. 2a). This secondary channel diverts a low percentage of the main channel flow discharge (about 10%). The gravel bar is totally covered for high flow conditions (over 110 m^3/s approximately). Actually, six patches were built with an initial objective to study inception motion of coarse particles in different initial stage of clogging (Camenen et al., 2015). Because the peak discharge was lower than expected, no movement of the gravel was observed (Camenen et al., 2015). The patch size was one square meter approximately; and the patches were located on the side of the secondary channel (cf. Fig. 2b). Preparation of the clean patches is detailed as follows: A surface of approximately one square meter was first excavated to a depth of approximately 10 cm. The resulting hole was then filled with gravels and pebbles between 4 and 10 cm in diameter. Coordinates (in the Lambert 93 system) of the four corners of each patch were measured using DGPS tool. A topographic survey of the gravel and secondary channel was also achieved before the flushing event.
During the flushing event, several measurements were performed to estimate hydro-sedimentary conditions over the patches. A system for video analysis was implemented using a camera fixed at the top of a telescopic

(a)

(b)

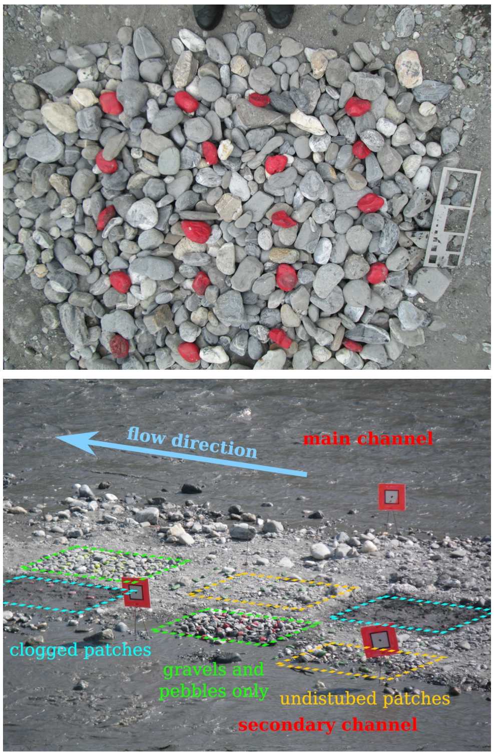

Figure 2: Photos of a clean patch (a) and of the disposition of all patches prepared for the experiment (b).

mast on the side embankment. The Large Scale Particle Image Velocimetry (LSPIV) method was used to measure the surface flow velocities during the event. Ground Reference Points (GRPs) were positioned in the view field using square targets (red and white) on the gravel bar and on the bank in order to make geometrical correction of the pictures (see Fig. 2b). The software Fudda-LSPIV (Le Coz et al., 2014) was eventually used to process the movies in order to get the velocity field and estimate the discharge within the secondary channel. 10 movies of 30 s were taken during the event, which corresponds to a movie every 40 mn in average. Two pressure gauges were installed upstream and downstream the secondary channel in order to obtain an estimation of the water level and slope within the secondary channel. Intense water sampling (every half an hour) was performed at both upstream and downstream ends of the secondary channel. Sediment concentration was measured for each sample using the filtration method and grain size analysis was made by laser diffractometry.

3. Experimental results

3.1 Discharge and sediment concentrations

The discharge was measured at the hydrometric station of Pontamafrey located 9 km upstream (see Fig. 3). It was estimated that the time for the wave to travel from Pontamafrey to Sainte-Marie-de-Cuine is $\Delta t_p = 45$ mn. Flushing operations are conducted yearly in June with the exception of years for which a large flood occurred previously. Since the same procedure is followed, similar discharge time series are generally observed with a first plateau at 80-100 m^3/s lasting approximately 4 hours and a second plateau at 120-130 m^3/s lasting approximately 4 hours. The 2014 flushing event was actually shorten with nearly no existence of the second plateau due to an incident in one of the dam reservoirs.

Concentration levels clearly follow the discharge time series (see Fig. 3). A plateau at 4 g/l is observed during the first plateau for Q followed by a pick at 12 g/l at the pick of discharge for which supercritical flow generally occurs in dam reservoirs. This may explain the much larger concentrations observed. However, these concentrations remain relatively low compared to previous flushing events (Antoine et al., 2011). Grain size analyses show that the composition of the suspension did not evolve significantly during the event ($d_{10} = 3\ \mu$m, $d_{50} = 17\ \mu$m, $d_{90} = 50\ \mu$m).

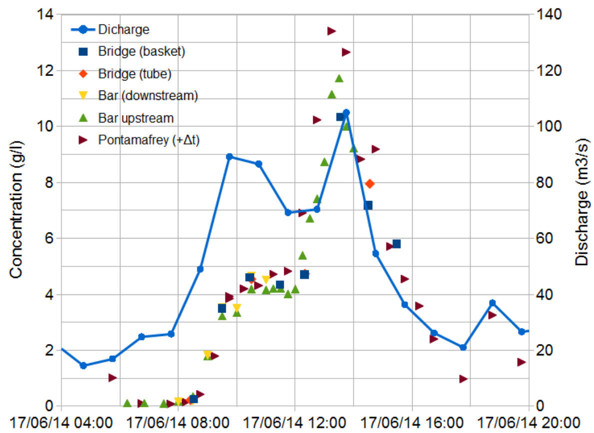

Figure 3: Water discharge and concentration time series measured upstream and downstream the gravel bar, 1 km downstream from a bridge and 10 km upstream at the hydrometric station of Pontamafrey with $\Delta t_p = 45$ mn.

3.2 Velocities and bed shear stresses

Surface velocity measurements were obtained using LSPIV method (Le Coz et al., 2014; Camenen et al., 2015). If a cross-section of the river bed is available, it is also possible to estimate the discharge assuming a ratio between the depth averaged velocity and the surface velocity of 0.85 (rough bed). Similarly, assuming a roughness length $k_s = 2d_{90} \approx 8$ cm, it is also possible to estimate the local and section averaged bed shear stress using the "law of the wall" method :

$$\tau_m = \rho C_f V^2 \qquad (1)$$

with $C_f = f(R_h, k_s)$ the friction coefficient, $R_h \approx H$ the hydraulic radius, H the mean water depth in the section, V the section-averaged velocity. Based on slope measurements, one can also compute section-averaged bed shear stress :

$$\tau_m = \rho g R_h S \qquad (2)$$

with ρ the water density, g the acceleration of gravity, and S the water slope. Section-averaged bed shear stress in the secondary channel is presented in Fig. 4 using both methods. Good agreement is observed between the two methods. Results from the LSPIV measurements are however very sensitive to the water level estimation, especially when water depths are shallow. This explains the very low value obtained at $t = 07{:}23$. In the zone over the patches, it was difficult to estimate the local bed shear stress. By extrapolation to what we could measure, we estimate it close to zero. However, some possible erosion of fine sediments could have been possible because of small waves propagating toward the gravel bar with a celerity of 10 cm/s approximately.

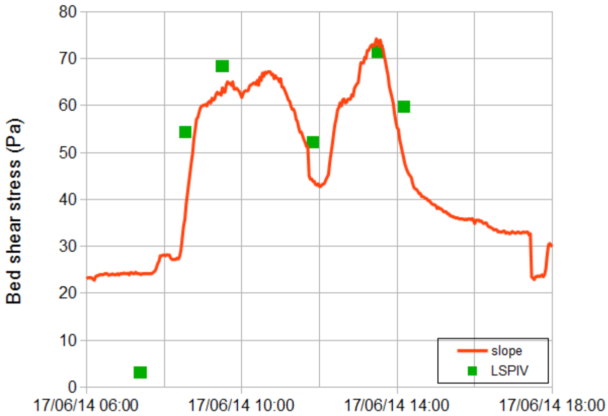

Figure 4: Mean bed shear stress in the secondary channel based on slope measurement and LSPIV measurement.

3.3 Fine sediment infiltration

A significant amount of fine sediments infiltrated the clean patch located close to the secondary channel (Figs. 2a and 5a). An estimation of the amount of fine sediments infiltrated was made using the following method (Fig. 5b and c): a surface $S \approx 0.2$ m^2 (0.45×0.45 m) was selected within the patch. All fine sediments infiltrated in the cobble layer ($\delta \approx 10$ cm) were collected in a basket. Coarse particles were taken out and cleaned in the same basket. Eventually, a sample of 5.23 kg was collected. Since some sandy particles may have been collected at the bottom of the layer, this sample was sieved at 0.5 mm. It remained 4.56 kg. When fine sediments are much smaller than coarse sediments, fines can percolate without getting trapped as they pass through the pore throats, therefore being deposited only on the top of coarse grains or on an eventual impermeable layer located under the gravel bed. In this situation, the bed is filled from the bottom upwards and tends to a relatively uniform distribution of fines over the bed depth. This infiltration mechanism that corresponds typically to our case is commonly known as unimpeded static percolation (Gibson et al., 2009; Evans and Wilcox, 2013). Assuming an initial porosity $p_{patch} = 0.4$ for the patch, and a porosity of $p_{fines} = 0.4$ for the fine sediments infiltrated, the maximum amount of fine sediments that could infiltrate the selected surface surface is :

$$M = \rho_s p_{patch}(1 - p_{fines})\delta S = 12.7 \text{ kg} \qquad (3)$$

This means that approximately 30% of the pores were clogged with fine sediments in $\Delta t_s \approx 60$ mn (time period for which the patch was underwater).

In Fig. 6, the grain size distributions of the suspended sediments and of the sediments infiltrated in the patch 3 are plotted. For the sediment in suspension, 5 classes of sediments (clay and silts) predominate (see Tab. 1).

The very same classes are observed for the sediments infiltrated but with different proportions. A class of poorly sorted fine sands with $d \approx 120$ μm is also present in the deposits. It clearly shows the grain sorting occurring over the bed during the infiltration process. Coarser particles with larger settling velocity do settle and infiltrate easier when bed shear stresses are very low. The presence of the fine sand class indicates that this sediment fraction trav-

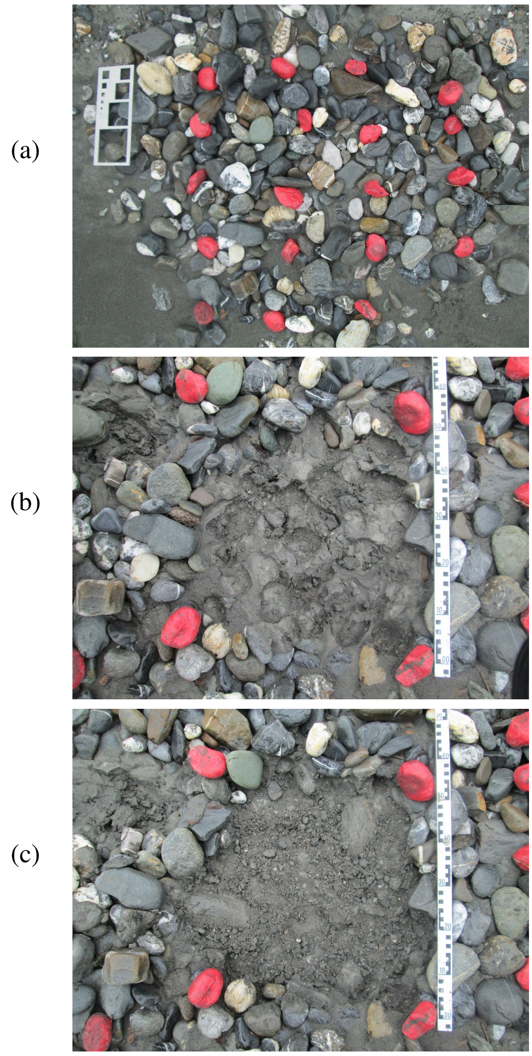

Figure 5: Photos of a clean patch after the flushing event (a), photos of the sampling surface after taking off pebbles (b) and cleaning all deposits (c).

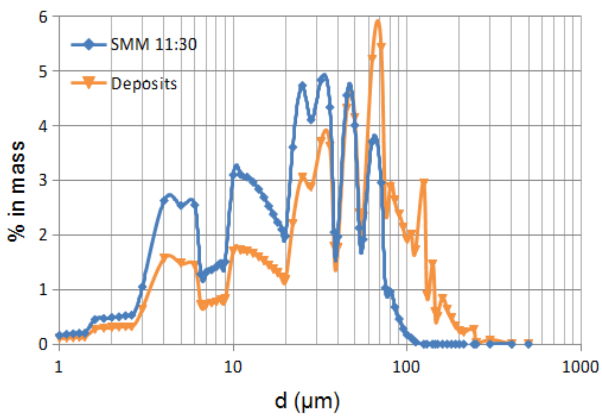

Figure 6: Comparison of the grain size distributions of the sediments in suspension (SSM 11:30) and the sediments infiltrated in the patch (deposits).

Table 1: Simplified grain size distribution of the sediments in suspension and estimation of the infiltrated flux (W_s : settling velocity; M_{dep} : mass infiltrated).

Class	d [μm]	% mass	W_s [m/s]	$M_{dep,mod}$ [kg]	$M_{dep,exp}$ [kg]
1	5	16	1.4×10^{-5}	0.02	0.45
2	12	35	8.0×10^{-5}	0.20	0.89
3	30	24	5.0×10^{-4}	0.85	0.79
4	45	15	1.1×10^{-3}	1.16	0.68
5	70	10	2.7×10^{-3}	1.99	1.14
6	120	0.1	7.0×10^{-3}	0.08	0.46
total		100		4.22	4.42

els in a graded suspension with concentration much larger close to the bottom. Surface water sampling on the side of the river do not allow to detect this class of sediments. It is possible to estimate the mass deposited (or infiltrated) from the theoretical settling flux :

$$M_{dep} = S\Delta t_s \sum W_{si} C_i \quad (4)$$

where W_{si} and C_i are the settling velocity (estimated using Camenen, 2007) and concentration for each class of sediment, respectively. We assumed here a constant total concentration $C = 10$ g/l during the period when the patch was submerged (see Fig. 3). As shown in Tab. 1, Eq. 4 yields overall good results for the estimation of the mass deposited. However, because of the high sensitivity of settling velocity to the grain size, such a computation leads to an overestimated sediment sorting. This may be explained by some possible flocculation effects for fine particles as well as some hindered effects for the coarser particles (see Tab. 1).

4. Conclusion

A field survey to study the dynamics of fine sediment dynamics in an alpine river during a flushing event is presented. It included flow velocity measurements and surface water sampling during the event and characteristics of the bed and reference patches before and after the event. Estimation of bed shear stress in the secondary channel using both pressure gauges and LSPIV measurements were in good agreement. An intense sampling frequency for the fine sediment in suspension is necessary for such event since the concentration values can change rapidly. A significant infiltration / deposition of fine particles was eventually observed in the patches. The infiltration rate was estimated at 0.1 g/s for $C \approx 10$ g/l resulting in a clogging of approximately 30% of the pores in one hour. Grain size analyses of both fine sediments in suspension and infiltrated sediments gave an interesting view of the fine sediment dynamics over the gravel bar, especially for the grain size interaction (flocculation, hindered effects). A similar experiment is planned for the 2015 flushing event with the objective of better estimating the inception of motion of coarse particles for different fine sediment contents.

References

Antoine, G., Camenen, B., Jodeau, M., and Esteves, M. (2011). Assessment of the suspended sediment load due to dam flushing along the Arc and Isère rivers, France. In *Proc. 7th IAHR symposium on River, Coastal and Estuarine Morphodynamics*, pages 1–10, Beijing, China. CD Rom.

Camenen, B. (2007). A simple and general formula for the settling velocity of particules in suspension. *J. Hydraulic Eng.*, 133(2):229–233.

Camenen, B., Herrero, A., Dramais, G., hollet, F., Le Bescond, C., Perret, E., and Berni, C. (2015). Field experiment on the dynamics of fine and coarse sediments over a gravel bar in an alpine river. In *Proc. 36th IAHR Congress*, The Hague, The Netherlands.

Diplas, P. (1994). Modelling of fine and coarse sediment interaction over alternate bars. *J. Hydrology*, 159:335–351.

Diplas, P. and Parker, G. (1992). Deposition and removal of fines in gravel-bed streams. In Billi, P., Hey, R. D., Thorne, C. R., and Tacconi, P., editors, *Dynamics of Gravel Bed Rivers*, pages 313–329. Wyley & Sons.

Eekhout, J. P. C., Hoitink, A. J. F., and Mosselman, E. (2013). Field experiment on alternate bar development in a straight sand-bed stream. *Water Resources Res.*, 49:1–12.

Evans, E. and Wilcox, A. C. (2013). Fine sediment infiltration dynamics in a gravel-bed river following a sediment pulse. *River Res. and Applications*, 30:372–384.

Gibson, S., Abraham, D., Heath, R., and Schoellhamer, D. (2009). Vertical gradational variability of fines deposited in a gravel framework. *Sedimentology*, 56:661–676.

Jaballah, M. (2013). *Alternate bar morphodynamics in an engineered mountainous river*. PhD thesis, C. Bernard University, Lyon, France. 196 p.

Jaballah, M., Camenen, B., and Paquier, A. (2014). Alternate bar development in an alpine river following engineering works. *Advances in Water Resources*, (accepted).

Jodeau, M. (2007). *Morphodynamique d'un banc de galets en rivière aménagée lors de crues [Gravel bar morphodynamics in an engineered river during high flow events]*. PhD thesis, Claude Bernard University, Lyon 1. (in French).

Konrad, C. P. (2002). Partial entrainment of gravel bars during floods. *Water Resources Res.*, 38:1104.

Lanzoni, S. (2000). Experiments on bar formation in a straight flume 2. graded sediment. *Water Resources Res.*, 36(11):3351–3363.

Le Coz, J., Le Boursicaud, R., Jodeau, M., Hauet, A., and Marchand, B. (2014). Image-based velocity and discharge measurements in field and laboratory river engineering studies using the free fudaa-lspiv software. In Schleiss, A. J., de Cesare, G., Franca, M. J., and Pfister, M., editors, *River Flow, Proc. 7th Int. Conf. on Fluvial Hydraulics*, Lausanne, Switzerland.

Lisle, T. E. and Hilton, S. (1999). Fine bed material in pools of natural gravel bed channels. *Water Resources Res.*, 35:1291–1304.

Lisle, T. E., Ikeda, H., and Iseya, F. (1991). Formation of stationary alternate bars in a steep channel with mixed-size sediment: a flume experiment. *Earth Surface Proc. & Landforms*, 16:463–469.